FINAL REPORT

Title: To Burn or Not to Burn: UAS Mapping of Tree-Level Foliar Moisture Content

JFSP PROJECT ID: 23-1-01-24

December 2024

Lauren E. Lad
Colorado State University

Camille S. Stevens-Rumann
Colorado State University

FIRESCIENCE.GOV
Research Supporting Sound Decisions

Contents

List of Tables

List of Figures

List of Abbreviations/Acronyms

1. FMC: Foliar Moisture Content
2. UAS: Uncrewed Aerial System
3. NDVI: Normalized Difference Vegetation Index
4. NDWI: Normalized Difference Water Index
5. PRI: Photochemical Reflectance Index
6. EP: Estes Park
7. RFL: Red Feather Lakes
8. DBH: Diameter at Breast Height
9. CBH: Canopy Base Height
10. GCP: Ground Control Point
11. NAD83 UTM 13N: North American Datum Universal Transverse Mercator zone 13 north
12. DTM: Digital Terrain Model
13. CHM: Canopy Height Model
14. NDVI2: Normalized Difference Vegetation Index 2 (uses 2^{nd} green band)
15. FMCI: Foliar Moisture Content Index
16. GNDVI: Green Normalized Difference Vegetation Index
17. NDRE: Normalized Difference Red Edge
18. AIC: Akaike Information Criterion
19. ME: Mean Error
20. RMSE: Root Mean Square Error
21. MLRM: Multiple Linear Regression Model

Acknowledgements

We acknowledge the Joint First Science Program and the Colorado Forest Restoration Institute for their generous funding of this project.

Abstract

Foliar moisture content (FMC) plays a crucial role in the arid, fire-adapted forests of the western US by influencing fire behavior, tree survival, and serving as a proxy for tree health. Management actions such as mechanical thinning and prescribed fire mitigate wildfire risk and improve forest health by reducing fuel connectivity, diversifying forest structure, and creating canopy gaps. These management actions could be improved by the targeted removal of moisture stressed trees during treatments. However, maps of FMC are not widely available at the tree-level, with no existing products to map FMC of western conifers at ultra-high resolution. This project focuses on the scalability of a laboratory-developed models of sapling FMC to develop an assess tree-level FMC in natural forest conditions. Specifically, we tested: Can existing FMC models accurately predict individual tree FMC using uncrewed aerial system (UAS) data? Field testing demonstrated that while laboratory-based models yielded low accuracies and a field-developed model only explained ~31% of the variation, the field model successfully classified trees into FMC categories (i.e. 10% lowest FMC, 90% highest FMC) with up to 89.8% accuracy. The successful classification demonstrates strong potential for UAS-based FMC mapping to inform management prescriptions. The integration of UAS-derived FMC classification into forest management decision workflows will enhance forest resilience and the adaptive capacity of managers.

Objectives

The objectives of this project were to 1) test the application of lab-developed models of drought stress and foliar moisture content from Lad et al. (2023) to natural forest systems, and 2) test the development of field-developed models of relative foliar moisture content. The successful completion of these objectives will improve our knowledge on the scalability of laboratory-based models and highlight any difficulties in scaling models from controlled settings to natural forests. Further, the successful completion of objective 2 will represent an advancement toward the application of site-specific models of foliar moisture content to inform resilience-minded forest management.

Background

Anthropogenic climate change is projected to increase the severity and intensity of drought across the Southwestern United States (Cook et al., 2015), particularly impacting western conifer forests through increasing temperatures, precipitation deficits (Cook et al., 2018), and decreased soil water storage (Liu et al., 2019, Bolinger et al., 2023). Between 2000 and 2019 CE, southwestern North America experienced its second driest two decades since 800 CE, resulting in a regional megadrought (Williams et al., 2020). This region is projected to experience continued trends of increasing temperatures coupled with variable precipitation (Bolinger et al., 2023). Temperature-driven decreases in soil water availability and higher plant water demand are contributing to plant-level physiological stress that reduces resilience to current and future drought (Breshears et al., 2005, Williams et al., 2012). Drought-induced physiological stress in trees reduces their resilience to fire and insect attacks (Sparks et al., 2024). Lower water availability affects trees by reducing foliar moisture content, nutrient uptake, and sap flux, all of which contribute to a tree's ability to withstand disturbances (Kreuzwieser & Gessler, 2010, Ryan, 2011). Drought stress is being compounded by stand density increases from historic norms (Mast et al., 1998) due to a legacy of fire suppression over the last century (Littell et al., 2016), which increases forest water demands and further stresses trees (Zhang et al., 2019). These compounding climate and management-induced demands on moisture availability then make forests more susceptible to drought-, fire-, and insect-induced mortality (Williams et al., 2013).

The interaction of drought and stand density stresses contribute to increases in mortality that can drive increases in fine, dead woody fuel accumulation (Ruthrof et al., 2016). Furthermore, increasing temperatures are driving decreases in surface fuel moisture, increasing the likelihood of ignition, fire hazard, and extreme fire days (Alexander & Cruz, 2013, Flannigan et al., 2015). Reduced moisture in both surface and canopy fuels increase the likelihood of fires transitioning from surface and ground fires into ladder fuels and the overstory, resulting in crown fires. Alterations to the drought, fire, and pest disturbance regimes, coupled with persistent drought in an era of climate change, may facilitate changes to forest successional pathways that result in ecosystem conversion following disturbance-induced mortality (Batllori et al., 2020, Coop et al. 2020). Thus, forest managers must consider the current climate and the projected increase in hot drought conditions, and work to maintain forest resilience in the face of increasing and compounding disturbances.

A major indicator of water availability in forests is foliar moisture content. Foliar moisture content (FMC) responds to vegetation health and is a surrogate for individual plant resilience to weather, climatic oscillations, and disturbances (Keyes, 2006, Zhang et al., 2019, Sparks et al., 2024). Further, FMC changes daily based on evapotranspiration and water loss, or through precipitation and water uptake (Groover, 2017). Beyond indicating the relative water content in plant material, FMC provides an estimate of fire risk and rate of spread (Jolly & Hadlow, 2012). Conventional measures of foliar moisture require the collection of foliage from each plant and a comparison of the foliage's dry and wet weight (Jolly & Hadlow, 2012), providing a sample of data to represent an entire population. The need to sample individual plants and oven-dry specimens limits data extent and delays the availability of foliar moisture observations after collection. As such, there is limited capacity to collect rapid, spatially continuous measures of foliar moisture, particularly across management scales (i.e., 10s to 100s hectares).

Satellite-based remote sensing can supplement field data collection to provide landscape-scale assessments of ecosystem stress (Lentile et al., 2006). Landsat and Sentinel collect multispectral imagery at 30 m and 20 m spatial resolution, respectively, and at 16- and 8-day return intervals. Plant water status is commonly assessed using spectral indices like the Normalized Difference Vegetation Index (NDVI, Rouse, 1974), Normalized Difference Water Index (NDWI, Gao, 1996), or thermal imagery (Pierce et al., 1990). These moderate-resolution satellite sensors average across multiple species, vegetation strata, and substrates within a single pixel, washing out plant and species level variation (Lentile et al., 2006). Thus, forest managers cannot easily leverage this moderate spatial resolution to inform management decisions about which trees to retain or cut during thinning operations.

Uncrewed Aerial Systems (UAS) offer a potential solution to these limitations as the temporal resolution can be controlled by users and the high spatial resolution imagery can be smaller than 3 cm (Perez-Rodriguez et al., 2019). Recent advances in UAS tree-level mapping have been successful in creating near-census maps of tree locations, heights, and diameters at breast height (DBHs) in dry, more open canopy conifer forests (Swayze et al., 2021, Tinkham et al., 2022). As these techniques become refined, UAS estimates of basal area and tree density achieve precisions of 5% to 10% (Tinkham & Woolsey, 2024) and spatial patterns match field collected data (Hanna et al., 2024). Additionally, several studies have attempted to use UAS multispectral and thermal imagery to estimate FMC or similar vegetation moisture and health metrics for agricultural and crop tree (i.e., cherry, olive, citrus, and chestnut trees) applications with varying success (Ezenne et al., 2019, Blanco et al., 2020, Garza et al., 2020, Grulke et al., 2020, Padua et al., 2020, Marques et al., 2023). In a Northeastern United States forest, Fraser & Congalton (2021) were able to classify between healthy, disturbed through either disease or pests, and degraded trees with 71% accuracy. In a European mixed-conifer forest, Abdollahnejad & Panagiotidis (2020) used multispectral imagery and a support vector machine classifier to classify leaf discoloration as an indicator of health with 84.7% accuracy. These studies show promise for tree-health assessments from UAS multispectral remote sensing, but no studies have examined the disturbance-adapted mixed-conifer forests of the Rocky Mountains, which are particularly at risk for future drought events.

Previous work on individual conifer tree FMC remote sensing used a laboratory setting to develop models to classify drought-stress status and predict continuous FMC from the spectral bands available on a consumer-grade multispectral UAS camera for both a short-needle and long-needle conifer species (Lad et al., 2023). This previous effort examined two conifer species at various levels of drought stress to classify drought status and predict FMC (Lad et al., 2023). Similar to studies monitoring crop FMC, Lad et al. (2023) found that indices such as the NDVI (Normalized Difference Vegetation Index) and PRI (Photochemical Reflectance Index), along with the red edge spectral range (700-720 nm) were the strongest predictors in modeling drought-stress in both short- and long-needle western conifers. D'Odorico et al. (2021) and Vicca et al. (2016) found that PRI was sensitive to real-time changes in photochemical efficiency, highlighting its utility for assessing tree health changes. Sparks et al. (2016) found that a pre- and post-burning differenced NDVI quantified vegetation stress and burn severity with a high correlation to photosynthetic activity (r2=0.73-0.85) following a laboratory burn. These modeling approaches, while promising, need to be validated through testing in mature forests of varying densities and drought conditions. Specifically, scaling these models to mature trees may present challenges to accurate quantification of FMC resulting from intra-tree variability or shadowing of lower branches.

Drought, as represented by decreased FMC, is and will continue to be a driving force of forest health and disturbance risk and recovery, underscoring its importance as a metric to describe forest conditions and to inform management actions. However, no comprehensive methods have yet been validated to predict tree-level FMC in forests. Lad et al. (2023) found that a logistic regression and multiple linear regression model using NDVI, PRI, and red edge spectra were effective in identifying drought stress of saplings. Thus, this study will further validate these models in two mature mixed-conifer forests in northern Colorado. Using the models developed by Lad et al. (2023) we answered the question: Can laboratory-developed models of drought stress be used to identify the gradient of drought stress in a mixed-species conifer forest?

Methods

Data Collection

To capture a gradient of FMC, this study was conducted at field sites with varying management histories and topographic complexities. The Estes Park (EP) site was dominated by a northwesterly aspect on a 7-60% slope covering 4.18 hectares and was hand thinned in 2012 to create an open mixed-conifer stand of ponderosa pine (*Pinus ponderosa* Lawson & C. Lawson) and Douglas-fir (*Pseudotsuga menziesii* (Mirb.) Franco var. *glauca* (Beissn.) Franco). The Red Feather Lakes (RFL) site was an untreated 6.0 hectacre area of open mixed-conifer forest of ponderosa pine and Douglas-fir occupying a small hill (slope=1-65%) with all aspects covered and featuring exposed rocky outcroppings (Figure 1).

Figure 1: UAS flight boundaries and derived true color imagery of the A) Red Feather Lakes (RFL) site and B) Estes Park (EP) site with the ESRI Outdoor base map.

Prior to FMC monitoring, field survey trees were selected in a random approach wherein 50 random points were generated at each site, with the nearest dominant or codominant ponderosa pine or Douglas-fir tree identified for sampling. Limiting to dominant and codominant trees was done to ensure reliable extraction from the UAS point cloud to allow for the testing of these drought models. The sample trees had their height, diameter at breast height (DBH), crown base height (CBH), and species recorded, along with their location using an Emlid Reach RS2+ real-time kinematic GPS (Emlid Tech Kft, Budapest, Hungary).

Each site was sampled two times, for a total of four collection dates and 199 foliar moisture samples (Table 1). On each collection date, needle collection began at approximately 10:00 and continued until 12:00 when UAS flights were conducted. Following UAS flights, any remaining trees were sampled, with all moisture samples collected within 2 hours of the UAS acquisition. Needle collection for each tree involved using loppers on an extending pole to clip bundles of needles in each cardinal direction and at varying tree heights. A minimum of four bundles were clipped from each tree and placed in a weighed and labeled plastic bag and stored in a cooler until they could be processed in the lab that afternoon. Variations in tree height and CBH meant that some samples could only be collected from the lower and middle third of the crown of some individuals. Testing was done on a subsample of trees where FMC could be assessed in the lower, middle, and upper third of individual crowns, with a paired t-test showing no significant differences (p=0.12).

Table 1: Mean (standard deviation) of sample trees across the three study sites along with dates of the FMC collections.

Site	**ponderosa pine**			**Douglas-fir**			**Collection Dates**	
	DBH (cm)	**Height (m)**	**CBH (m)**	**DBH (cm)**	**Height (m)**	**CBH (m)**		
Estes Park (EP)	29.4 (7.7)	13.9 (2.2)	3.5 (1.0)	30.7 (12.4)	14.4 (3.5)	2.0 (1.0)	July 27	Sept. 18
Red Feather Lakes (RFL)	29.0 (11.3)	10.2 (3.1)	2.4 (1.2)	22.3 (6.8)	9.3 (2.9)	0.7 (0.5)	July 25	Oct. 16

In the lab, bundles were removed from their plastic bag, stripped their needles and cones from the branch, and added only the needles back to the bag. The wet needle weight for each tree was measured by subtracting the plastic bag's weight from the needles in the bag. All wet weights were recorded within six hours of field sample collection. Then, needles were transferred to paper bags and dried in an oven at 105 degrees Fahrenheit for at least 48 hours, or until the dry weight had stabilized (Matthews, 2010). Once dry, the dry weight of each sample was measured by weighing the dried needles on a tared scale. All weights were recorded using an OHAUS scale with a precision of 0.01 grams (OHAUS Corporation, Parsippany, NJ, USA). The FMC of each sample was calculated using equation 1 (Jolly & Hadlow, 2012).

$$Foliar\ Moisture\ Content = \frac{(Wet\ Weight - Dry\ Weight)}{Dry\ Weight}\ x\ 100 \qquad [1]$$

UAS flights were conducted as close to 12:00 as possible to align with the sun's peak and reduce shadowing in the imagery. Acquisitions were conducted using a DJI Matrice 210V2 (DJI, Shenzhen, China) with a Micasense 10-band Dual-Camera system attached (Micasense, Seattle, WA, USA) and lasted an average of 20 minutes at each site. Prior to takeoff and immediately after landing, manual captures were taken of the Micasense reflectance panels. These images allowed us to capture 100% reflectance and were used to correct for inconsistencies in lighting during the flights. All flights used a serpentine flight pattern at 90 m above ground level and at a speed of 6 m s^{-1} with 85% forward and 80% cross-track image overlap. The Micasense system captured 10-band multispectral imagery (Table 2) at 6.3 cm resolution. Ground control points (GCPs) were used at each site to ensure spatial accuracy of image alignment. These GCPs were chosen based on visibility from above, spacing across the sites, and had their locations recorded using an Emlid Reach RS2+ real-time kinematic GPS (Emlid Tech Kft, Budapest, Hungary). The GCPs had a reported average horizontal and vertical root mean square error of 0.038 m and 0.077 m, respectively.

Table 2: List of bands available on the Micasense Dual-Camera System and the wavelengths covered by each band.

MicaSense Band	**MicaSense λ**
Blue	430-458 nm
Blue 2	465-485 nm
Green	550-570 nm
Green 2	524-538 nm
Red	663-673 nm
Red 2	642-658 nm
Red Edge 1	712-722 nm
Red Edge 2	700-710 nm
Red Edge 3	731-749 nm
Near Infrared	820-860 nm

UAS Image Processing

For each of the four acquisitions, UAS images were processed in Agisoft Metashape version 1.6.4 (Agisoft LLC., St. Petersburg, Russia) using the Structure from Motion algorithm with Mild Depth Map Filtering and High-Quality generation parameters. These settings were used to maximize individual tree extraction accuracy based on the findings of Tinkham and Swayze (2021). Photos of the reflectance panels were used to calibrate image spectral reflectance and correct for lighting inconsistencies due to clouds and sun angle.

The GCP locations were imported to Metashape and iteratively georeferenced using a minimum of 10 photos per GCP, resulting in a median (s.d.) root mean square error of 7.3 (5.2) cm, 5.8 (3.5) cm, and 0.8 (0.5) cm for X, Y, and Z locations, respectively across all sites and collections. Once GCPs were georeferenced, UAS photos were aligned to produce approximately 5-8 million tie points as well as an orthomosaic and dense point cloud with information for the 10 spectral bands attached. The orthomosaics had a final pixel resolution of 6.3 cm. Before export, pixel and point values were converted from digital number to reflectance by dividing each band value by 32,768 following the recommendation of the camera manufacturer (MicaSense Seattle, WA, USA). Then, orthomosaics and point clouds were exported as GeoTiffs and LAS files, respectively, for each flight date in the North American Datum 1983 UTM Zone 13 North (NAD83, UTM 13N) projected coordinate system. These data were then imported into R for analysis.

To extract individual trees and tree crowns, point clouds and orthomosaics were processed in RStudio version 4.3.2 (R Core Team, 2022). Following the point cloud processing steps from Tinkham & Woolsey (2024), point clouds were processed using the cloud2trees package (Woolsey, 2024) which integrates the lasR (Roussel, 2024) and lidR packages (Roussel et al., 2020, Roussel & Auty, 2024). First, raw point clouds were denoised which involved classifying isolated points and dropping them, as well as duplicate points, from the point cloud. Then, we classified ground points and generated a digital terrain model (DTM) with 1.0 m resolution using Delaunay triangulation and pit fill. This allowed us to height normalize the point cloud and generate a canopy height model (CHM) at 0.10 m resolution. To locate individual trees, we used a variable window function [Equation 2] as proposed by Creasy et al. (2021) and the locate_trees function from the lidR package to identify all tree tops that were at least 2 meters tall. Then, we delineated tree crowns using the marker-controlled watershed function of the ForestTools package (Plowright, 2024). Finally, we spatially joined the tree tops with the tree crowns following the methods of Tinkham et al. (2022). The outputs of these steps included a CHM and DTM raster, individual tree crown polygons, and tree location points which included the calculated height.

$$Variable\ Window\ Radius = 0.3 + CHM\ Value * 0.1 \qquad [2]$$

The tree location points were spatially matched to field-collected tree locations following the methods of Tinkham et al. (2022). This spatial matching process used a maximum search distance of 5 m and a maximum height error of 4 m to identify the nearest UAS trees to the field trees using the sf package (Pebesma, 2018). The UAS tree within the search distance with the smallest height error was then assigned to the field tree as a match. These matches were used with the st_intersects function from the sf package to extract the nearest individual tree crown polygon. Then, using the individual tree crown polygons and 10-band orthomosaics, we derived each pixel's spectral values for each of the 10 bands within each crown polygon using the exact_extract function of the exactextractr package (Baston, 2024). These values were normalized to the reflectance scale by dividing each cell value for a given band by the global maximum of that respective band (Micasense). Then, using the normalized cell values we calculated NDVI2 (Equation 3), PRI (Equation 4), and FMCI (Equation 5), and extracted Red Edge 3 values for all pixels. Raster values within each polygon were further summarized as the mean, median, 10th, 20th, 25th, 30th, 40th, 60th, 70th, 75th, 80th, and 90th percentile band and index values for each tree crown. The band and index values were appended to the field tree lists to be used as predictor variables in the multiple linear regression model developed by Lad et al. (2023). We also evaluated species, Julian date, and site as potential predictor variables.

$$NDVI2 = \frac{NIR - Red2}{NIR + Red2} \qquad [3]$$

$$PRI = \frac{Green2 - Green}{Green2 + Green} \qquad [4]$$

$$FMCI = \frac{RedEdge3 - NIR}{RedEdge3 + NIR} \quad [5]$$

Modeling and Data Analysis

After summarizing predictor variables, we tested the Multiple Linear Regression Model (MRLM; Equation 6) from Lad et al. (2023) which used NDVI2, PRI, FMCI, and the RedEdge3 band as predictor variables. This modeling approach applied the stats package in base R (R Core Team, 2023). We tested each summarization technique (i.e., mean, median, X^{th} percentile, etc.) on these four variables, fitting 12 to the summarized metrics, and compared their accuracy in predicting observed FMC using Pearson's correlation, mean error (ME), and root mean square error (RMSE). Then, we performed a paired t-test to determine the difference between the mean observed FMC and the mean model-predicted FMC. Finally, we computed ranks for the observed and predicted values and tested their difference with Spearman's rank correlation.

$$FMC\% = -226.61 + 138.64 \times NDVI2 + 611.92 \times RedEdge3 + 851.31 \times FMCI + 1039.63 \times PRI \quad [6]$$

To identify potential differences between the lab model and the optimal prediction of FMC using field scale data, we also fit a series of multiple linear regression models using the UAS-derived tree-level spectral bands and indices, along with species and Julian date to predict FMC. We fit RandomForest models to each of the 12 sets of summarization metrics (e.g., 10^{th}, 20^{th}, 30^{th} percentile, etc.) to predict FMC using the RandomForest R package (Liaw & Wiener, 2002). The models included the tree-level summary metrics for the ten spectral bands and nine spectral indices. These spectral indices included NDVI, NDVI2, PRI, FMCI, Normalized Difference Wetness Index (NDWI; Equation 7), Green Normalized Difference Vegetation Index (GNDVI; Equation 8), and Normalized Difference Red Edge (NDRE; Equation 9). The best summarization metric was identified as the model with the greatest variance explained (R^2) by the RandomForest regression model.

$$NDWI = \frac{Green - NIR}{Green + NIR} \quad [7]$$

$$GNDVI = \frac{NIR - Green}{NIR + Green} \quad [8]$$

$$NDRE = \frac{NIR - RedEdge1}{NIR + RedEdge1} \quad [9]$$

For the set of spectral bands and indices identified as the best summarization approach using RandomForest, we tested variable correlation to remove any highly (i.e., >70%) collinear variables. The reduced non-collinear set of predictors was used to generate a final multiple linear regression model of FMC using the stats R package (R Core Team, 2023). The model was reduced using a forward-backward stepwise approach to minimize the Akaike Information Criterion (AIC) using the olsrr R package (Hebbali, 2020). Utilizing the reduced variable set, we estimated predictor coefficients and their 95% confidence intervals using bootstrapping with 1,000 repetitions using the boot R package (Davison & Hinkley, 1997; Canty & Ripley, 2022), allowing us to check uncertainty and model consistency. To further analyze the best-fitting model, the predicted and observed values were ranked within the distribution, and the accuracy of placing trees into two categories was assessed. The intention of this was to mimic how a manager might target the 30% or 40% most drought-stressed trees. The average accuracy of splitting predictions into two bins was assessed if the method was used to identify the 10%, 20%, 30%, 40%, and 50% most drought-stressed trees.

Results & Discussion

Field-collected FMC was approximately normally distributed when examined across all sites and dates (Figure 2). The observed FMC values ranged from 73% to 126%, with an average of 98.4%. FMC across the four dates was bimodally distributed, but the range of FMC values tended to narrow through time. Additionally, the FMC values at EP tended to be higher when compared to RFL, and there were generally higher values for Douglas-fir than ponderosa pine (Figure 2).

Spectral reflectance of bands and indices were also compared across Julian dates to examine the importance of the collection date (Figure 3). Most spectral bands exhibited low variation between Julian dates, except for the first data collection which consistently had greater reflectance levels. Within a single collection date, bands in the red and red edge portion of the spectrum featured greater variability and wider interquartile ranges than bands with shorter wavelengths. The near-infrared indices (NDVI2 and FMCI) exhibited lower mean values for the RFL collections (first and last Julian date) compared to the EP collections, with there being much more consistency in the PRI values between dates, but less within site variation.

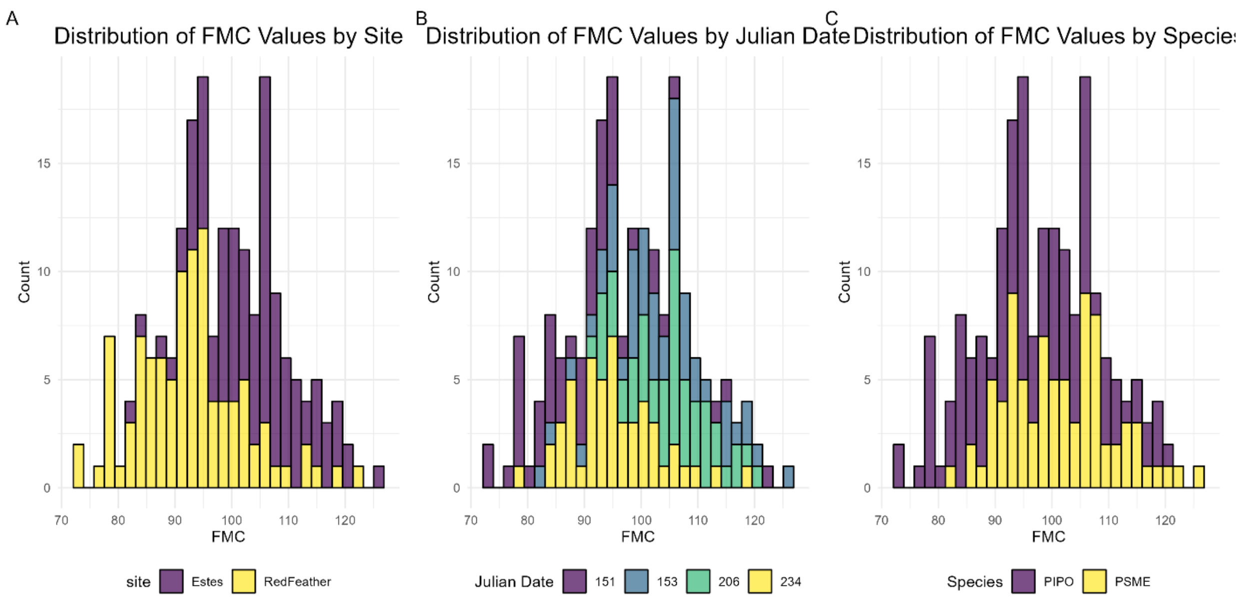

Figure 2: Histograms of foliar moisture content values across the four collections at the Red Feather Lakes (RFL) and Estes Park (EP) sites separated into A) distribution by site, B) distribution by Julian date, and C) distribution by species.

Comparing the 12 sets of MLRM predictions from Lad et al. (2023) against observed FMC values found that the mean reflectance achieved the highest Pearson's correlation, while the 90th percentile achieved the lowest ME and RMSE (Table 3.3). A paired t-test of the observed and predicted values found no significant difference between means (p=0.57) using the 90th percentile technique, but the mean technique was significantly different (p<0.05). Across the 12 summarized models, the correlation generally remained stable but using lower percentiles of within canopy values had higher correlation and there was a slight decline in correlation at higher percentiles. However, the ME and RMSE decrease with the use of higher percentiles, suggesting an increase in accuracy of the predicted values. Testing the ranking of the predicted FMC values from the mean and 90th percentile models against the observed rankings using Spearman's rank correlation showed that both models similarly captured the gradient of FMC values (Spearman's rank Correlation=45.06 and 44.07, respectively).

Figure 3: Boxplot of spectral band and index distribution within surveyed tree crowns colored by Julian date.

Table 3: Accuracy of each summarization metric tested in applying the multiple linear regression model from Lad et al. (2023).

Summarization Technique	Pearson's Correlation	Mean Error	Root Mean Square Error
Mean	43.70	203.77	238.44
Median	41.38	197.08	237.00
10^{th} Percentile	42.06	411.86	431.77
20^{th} Percentile	42.19	345.18	368.12
25^{th} Percentile	42.30	317.33	342.09
30^{th} Percentile	42.12	291.50	318.50
40^{th} Percentile	41.67	242.94	275.42
60^{th} Percentile	41.22	153.16	202.91
70^{th} Percentile	40.94	109.54	173.04
75^{th} Percentile	40.83	86.89	159.92
80^{th} Percentile	40.51	63.14	148.40
90^{th} Percentile	39.81	5.53	135.66

The lack of high accuracy in the lab-developed MLRM could be the result of scaling and summarization mismatches. In the lab, pure individual sapling spectral values were collected using three plant probe samples across the crown, while in the field, tree spectral values were collected as pixels across the entire crown, with values primarily reflecting the top 2D profile of the crown. To account for the mixture of foliage, branch, and background substrate captured in the UAS pixels, we attempted to account for these collection approach differences by testing summarization techniques. However, the UAS imagery also contended with greater spectral variability in mature crowns as, even within extracted polygons, there are differences in crown shading/illumination. This all contributes to the relatively narrow spectral distribution of the laboratory saplings (Figure 4) compared to the UAS imagery (Figure 3). The young needles (i.e., less than two years old) on the laboratory saplings likely reflect more light (Rock et al., 1994) compared to the older (i.e., up to five years old) needles assessed in the field. Comparing the lab spectral data from Lad et al. (2023) against this study's UAS data shows a much lower and narrower range of near-infrared values from the lab data. The lack of variability in the training data for the lab MLRM likely contributed to a lack of model fit when predicting using field values that featured higher levels of variability, as well as higher reflectance values in general.

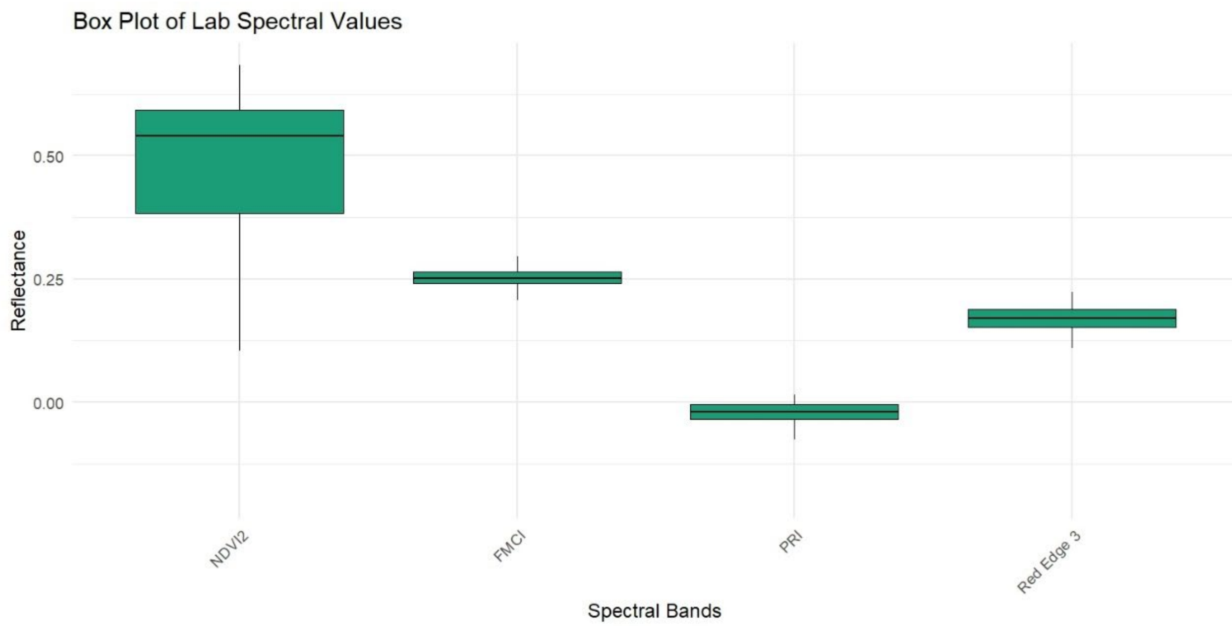

Figure 4: Distribution of band spectral values collected during Lad et al. (2023) and applied in the lab multiple linear regression model.

RandomForest identified that using the 80th percentile of tree-level summarized spectral bands and indices provided the most predictive power. In our testing of summarization approaches, species was a significant predictor of FMC in ten out of twelve of the RandomForest models, highlighting its utility. The final reduced multiple linear regression model developed on the field data retained species and the within crown 80th percentile values of NDVI2 and FMCI as predictors and resulted in an adjusted R^2 of 31.02 ($p<0.05$) with a residual standard error of 8.98% FMC (Figure 5). Predicted FMC increased as the index score increased for both NDVI2 and FMCI (Table 4). Additionally, species was significant with Douglas-fir increasing the intercept by 4.2% FMC over ponderosa pine.

Table 4: Final reduced multiple linear regression model output table.

	Coefficient	Confidence Interval	Standard Error	T value	p-value
Intercept	89.71	75.59, 100.74	4.38	20.50	<0.05
Douglas-fir	4.20	1.15, 6.68	1.31	3.22	<0.05
NDVI2_p80	23.67	10.75, 41.67	4.67	5.07	<0.05
FMCI_p80	35.58	21.75, 55.62	8.72	4.43	<0.05

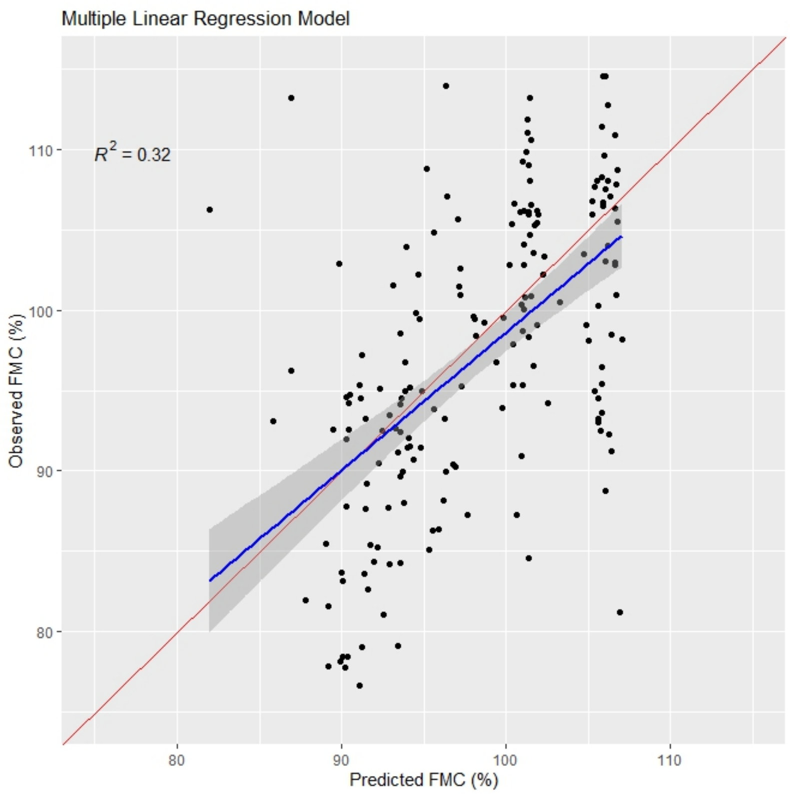

Figure 5: Observed and predicted foliar moisture content from a multiple linear regression model using Species and the 80th percentile values of NDVI2 and FMCI as predictor variables.

To test the utility of the model in thresholding the predictions to inform management decisions, we ranked the predicted and observed values and subset them into binary classes representing the lower 50% of FMC and higher 50% of FMC. This single split achieved an accuracy of 75.5% with bin standard errors of 2.9% each. Repeating this process to include splits identifying the 10%, 20%, 30%, 40%, and 50% most drought stressed trees resulted in an average accuracy of 81.40%, with accuracy declining from 89.8% for the 10/90 split to 75.5% for the 50/50 split. Similarly, the smaller bin identifying the more drought-stressed trees had an average class standard error of 2.2% that went from 1.3% to 2.9% as the bin increased from 10% to 50% of the predictions. The larger bin inversely declined from 3.8% to 2.9% as the bin decreased from 90% to 50%, with an average of 3.4%. Predicted bins were statistically significant (i.e., $p<0.05$) when identifying the 30%, 40%, and 50% most drought stressed trees, but not when the threshold was set to identify the 10% ($p=0.56$) or 20% ($p=0.17$) most drought stressed trees.

When UAS derived values were applied to the prediction of FMC, the lab developed MLRM achieved relatively low prediction accuracy. The new multiple linear regression model fit to the UAS data predicted FMC values that were successfully classified using a threshold to identify trees with higher vs lower drought-stress with 81.4% accuracy. While exact predictions of FMC had a mean error of ~9%, it is likely more important to capture the gradient of drought-stress as FMC is known to change rapidly in the field, with ponderosa pine previously shown to vary up to 34% diurnally in the summer with daily minima occurring in the morning and shortly after noon (Philpot, 1965). These temporal fluctuations likely mean that a prediction of FMC at a single time point does not necessarily represent the health of an individual tree. However, mid-day acquisitions would facilitate capturing the lowest within-tree relative FMC, while reducing shadowing in imagery. Further, FMC for Douglas-fir and ponderosa pine is typically between

100% and 130% in the summer with old foliage having values commonly under 100% (Keyes, 2006). However, our field observed average FMC across summer collection dates was 98%, with many trees below 90% FMC. The EP site had consistently higher FMC values, potentially resulting from this site being in a post-treatment condition, while the RFL site has high forest density and has not been treated or disturbed in the last 100 years.

The 81.4% classification accuracy in identifying the most drought-stressed trees is slightly lower than previous studies attempting to classify tree health status using UAS multispectral imagery in orchards (healthy/unhealthy 97.52%; Jemaa et al, 2023), and in mixed broadleaf-conifer forests (live/dead/beetle infested 84.71%; Abdollahnejad & Panagiotidis, 2020), but no studies have thus far identified relative health of western US mixed-conifer forests at the individual tree scale. As UAS sensor technology continues to advance and attempts to integrate hyperspectral, short-waver infrared, or thermal imagery, model accuracy of FMC and other health metrics should continue to improve. Using a hyperspectral camera, Näsi et al. (2018) classified bark beetle stress into health/infested/dead classes in an urban forest with 81% accuracy. Physiological indicators of tree health, such as stomatal conductance and leaf water potential, can also be captured using hyperspectral and thermal imagery with crown temperature showing a strong correlation with stomatal conductance (Zarco-Tejada et al., 2012). UAS show strong potential for the early detection of tree moisture stress and models should consider ecosystem-specific physiology, such as species composition and morphology, and abiotic factors such as topography and hydrology (Ewane et al., 2023). The wide range of applications of UAS imagery for vegetation health assessment is critical for the maintenance and restoration of forest resilience and should continue to be explored in the context of disturbances and global change ecology. Future research aiming to apply UAS imagery for tree health assessments should consider sensor cost, sensor spectral and spatial resolution, and site variability of biotic and abiotic factors when choosing the UAS that will be flown.

Implications for Management

Forest FMC is an important indicator of forest resilience and the relative distribution of FMC within a site can highlight areas for targeted management actions. Our models of site-specific relative FMC could be applied to forest sites and provide managers with relative tree stress to inform targeted thinning and prescribed fire operations, resulting in subsequent increases in growth and resilience against drought. Specifically, our models can produce maps of the 20% most stressed or healthy trees on a site. These maps could be combined with tree size and spatial arrangement maps and be used to inform managers of areas to target to increase the vertical and horizontal complexity of their forests, while prioritizing the retention of the site's most resilient individuals (Churchill et al., 2013). Additionally, these models could be used to evaluate sites post-thinning to examine changes to moisture content of the remaining trees (North et al., 2009). By connecting our model of tree-level FMC with ecologically-informed management, we can increase the information available for adaptive management that balance forest resilience and fire risk reduction.

In fire-dependent forests, the application of our models could guide ignition strategies, allowing managers to adjust ignition line distance to control fireline intensity based on burn-specific mortality objectives. By providing managers with near-real-time access to overstory fuel conditions, we can expand the information available to managers while they make fire planning decisions. Further, in areas with an increasing occurrence of short-interval fires, these models could be applied to assess the resilience of surviving trees after initial fires and inform thinning and refugia management to increase resistance to subsequent disturbances.

There is strong potential to operationalize these models and inform site-specific management decisions. These models could be integrated into management workflows either in the planning or evaluation stages. To integrate these models into planning, UAS data could be collected on a site prior to treatment. This data could be processed into individual tree spectral values to be input into relative FMC models. In combination with tree size and distribution maps, relative FMC models of the overstory trees could identify target trees for retention (i.e., the 50% highest FMC trees) to maintain site resilience. Then, managers could compare potential treatment maps that combine tree spatial distribution and site health models to make informed decisions for thinning operations. Finally, UAS data could be collected post-treatment to examine changes to relative site FMC and examine management-induced improvements to individual tree FMC.

Future Research

Future research will focus on operationalizing our model to provide managers with site-specific maps of relative tree stress. To adapt our model for application, species classification models will be integrated into the workflow. Additionally, individual trees were not consistent in their rank through collection dates, highlighting a need to examine seasonality of FMC and the importance of collection timing to ensure FMC rankings reflect relative health accurately. Further testing of these models on intermediate size trees, and those shaded out by the overstory, is needed as these intermediate trees are likely the target of management actions aiming to reduce forest density and fuel connectivity. Finally, model validation will continue at additional forest sites in Northern Colorado to examine model transferability.

Conclusions

Our analysis identified the most stressed trees at two sites in northern Colorado with ~80% accuracy, representing a significant advancement in the tools available for adaptive management in a semi-arid environment. As aridity is expected to increase in the coming years, this model provides valuable insights to guide targeted treatments aimed at enhancing forest resilience to future disturbances. Managers could integrate this model with site-specific knowledge and maps of tree composition and distribution to make fully informed decisions. By identifying areas with historically persistent openings, managers can pinpoint locations where infilling trees are likely drought-stressed due to soil moisture and nutrient limitations (Bond & Keeley, 2005). This would allow managers to prioritize areas for intervention and restoration while accounting for both overstory relative FMC, as well as underlying soil conditions. The operationalization of these models would allow for the production of site-specific maps of FMC distribution, allowing managers to target specific trees for either removal, for fire risk reduction, or retention, to build site resilience. Future work should evaluate the accuracy of this model for predicting relative FMC of additional species and in different elevation zones both within Colorado, and across the western United States.

References

Abatzoglou, J. T., & Williams, A. P. (2016). Impact of anthropogenic climate change on wildfire across western US forests. *Proceedings of the National Academy of Sciences*, *113*(42), 11770–11775. https://doi.org/10.1073/pnas.1607171113

Abdollahnejad, A., & Panagiotidis, D. (2020). Tree Species Classification and Health Status Assessment for a Mixed Broadleaf-Conifer Forest with UAS Multispectral Imaging. *Remote Sensing*, *12*(22), Article 22. https://doi.org/10.3390/rs12223722

A. Liaw and M. Wiener (2002). Classification and Regression by randomForest. *R News 2*(3), 18-22.

Agee, J. K., & Skinner, C. N. (2005). Basic principles of forest fuel reduction treatments. *Forest Ecology and Management*, *211*(1), 83–96. https://doi.org/10.1016/j.foreco.2005.01.034

Allen, C. D., Macalady, A. K., Chenchouni, H., Bachelet, D., McDowell, N., Vennetier, M., Kitzberger, T., Rigling, A., Breshears, D. D., Hogg, E. H. (Ted), Gonzalez, P., Fensham, R., Zhang, Z., Castro, J., Demidova, N., Lim, J.-H., Allard, G., Running, S. W., Semerci, A., & Cobb, N. (2010). A global overview of drought and heat-induced tree mortality reveals emerging climate change risks for forests. *Forest Ecology and Management*, *259*(4), 660–684. https://doi.org/10.1016/j.foreco.2009.09.001

Anderegg, W. R. L., Anderegg, L. D. L., & Huang, C. (2019). Testing early warning metrics for drought-induced tree physiological stress and mortality. *Global Change Biology*, *25*(7), 2459–2469. https://doi.org/10.1111/gcb.14655

Anderegg, W. R. L., Anderegg, L. D. L., Kerr, K. L., & Trugman, A. T. (2019). Widespread drought-induced tree mortality at dry range edges indicates that climate stress exceeds species' compensating mechanisms. *Global Change Biology*, *25*(11), 3793–3802. https://doi.org/10.1111/gcb.14771

Anderegg, W. R. L., Flint, A., Huang, C., Flint, L., Berry, J. A., Davis, F. W., Sperry, J. S., & Field, C. B. (2015). Tree mortality predicted from drought-induced vascular damage. *Nature Geoscience*, *8*(5), 367–371. https://doi.org/10.1038/ngeo2400

Andrews, C. M., D'Amato, A. W., Fraver, S., Palik, B., Battaglia, M. A., & Bradford, J. B. (2020). Low stand density moderates growth declines during hot droughts in semi-arid forests. *Journal of Applied Ecology*, *57*(6), 1089–1102. https://doi.org/10.1111/1365-2664.13615

Baston, D. exactextractr: fast extraction from raster datasets using polygons. R package version 0.10.0, https://github.com/isciences/exactextractr

Batllori, E., Lloret, F., Aakala, T., Anderegg, W. R. L., Aynekulu, E., Bendixsen, D. P., Bentouati, A., Bigler, C., Burk, C. J., Camarero, J. J., Colangelo, M., Coop, J. D., Fensham, R., Floyd, M. L., Galiano, L., Ganey, J. L., Gonzalez, P., Jacobsen, A. L., Kane, J. M., … Zeeman, B. (2020). Forest and woodland replacement patterns following drought-related mortality. *Proceedings of the National Academy of Sciences*, *117*(47), 29720–29729. https://doi.org/10.1073/pnas.2002314117

Blanco, V., Blaya-Ros, P. J., Castillo, C., Soto-Vallés, F., Torres-Sánchez, R., & Domingo, R. (2020). Potential of UAS-Based Remote Sensing for Estimating Tree Water Status and Yield in Sweet Cherry Trees. *Remote Sensing*, *12*(15), Article 15. https://doi.org/10.3390/rs12152359

Boča, A., Van Miegroet, H., & Gruselle, M.-C. (2014). Forest Overstory Effect on Soil Organic Carbon Storage: A Meta-analysis. *Soil Science Society of America Journal*, *78*(S1), S35–S47. https://doi.org/10.2136/sssaj2013.08.0332nafsc

Bolinger, R., Lukas, J., Schumacher, R., & Goble, P. (2023). Climate change in Colorado. https://hdl.handle.net/10217/237323

Bond, W. J., & Keeley, J. E. (2005). Fire as a global 'herbivore': The ecology and evolution of flammable ecosystems. *Trends in Ecology & Evolution*, *20*(7), 387–394. https://doi.org/10.1016/j.tree.2005.04.025

Breshears, D. D., Cobb, N. S., Rich, P. M., Price, K. P., Allen, C. D., Balice, R. G., Romme, W. H., Kastens, J. H., Floyd, M. L., Belnap, J., Anderson, J. J., Myers, O. B., & Meyer, C. W. (2005). Regional vegetation die-off in response to global-change-type drought. *Proceedings of the National Academy of Sciences*, *102*(42), 15144–15148. https://doi.org/10.1073/pnas.0505734102

Churchill, D. J., Larson, A. J., Dahlgreen, M. C., Franklin, J. F., Hessburg, P. F., & Lutz, J. A. (2013). Restoring forest resilience: From reference spatial patterns to silvicultural prescriptions and monitoring. *Forest Ecology and Management*, *291*, 442–457. https://doi.org/10.1016/j.foreco.2012.11.007

Cook, B. I., Ault, T. R., & Smerdon, J. E. (2015). Unprecedented 21st century drought risk in the American Southwest and Central Plains. *Science Advances*, *1*(1), e1400082. https://doi.org/10.1126/sciadv.1400082

Cook, B. I., Mankin, J. S., & Anchukaitis, K. J. (2018). Climate Change and Drought: From Past to Future. *Current Climate Change Reports*, *4*(2), 164–179. https://doi.org/10.1007/s40641-018-0093-2

Coop, J. D., Parks, S. A., Stevens-Rumann, C. S., Crausbay, S. D., Higuera, P. E., Hurteau, M. D., ... & Rodman, K. C. (2020). Wildfire-driven forest conversion in western North American landscapes. *BioScience*, *70*(8), 659-673. https://doi.org/10.1093/biosci/biaa061

Dash, J. P., Pearse, G. D., & Watt, M. S. (2018). UAV Multispectral Imagery Can Complement Satellite Data for Monitoring Forest Health. *Remote Sensing*, *10*(8), Article 8. https://doi.org/10.3390/rs10081216

Davis, K. T., Peeler, J., Fargione, J., Haugo, R. D., Metlen, K. L., Robles, M. D., & Woolley, T. (2024). Tamm review: A meta-analysis of thinning, prescribed fire, and wildfire effects on subsequent wildfire severity in conifer dominated forests of the Western US. *Forest Ecology and Management. 561: 121885.*, *581*, 121885. https://doi.org/10.1016/j.foreco.2024.121885

D'Odorico, P., Schönbeck, L., Vitali, V., Meusburger, K., Schaub, M., Ginzler, C., Zweifel, R., Velasco, V. M. E., Gisler, J., Gessler, A., & Ensminger, I. (2021). Drone-based physiological index reveals long-term acclimation and drought stress responses in trees. *Plant, Cell & Environment*, *44*(11), 3552–3570. https://doi.org/10.1111/pce.14177

Earles, J. M., North, M. P., & Hurteau, M. D. (2014). Wildfire and drought dynamics destabilize carbon stores of fire-suppressed forests. *Ecological Applications*, *24*(4), 732–740. https://doi.org/10.1890/13-1860.1

Ewane, E. B., Mohan, M., Bajaj, S., Galgamuwa, G. A. P., Watt, M. S., Arachchige, P. P., Hudak, A. T., Richardson, G., Ajithkumar, N., Srinivasan, S., Corte, A. P. D., Johnson, D. J., Broadbent, E. N., de-Miguel, S., Bruscolini, M., Young, D. J. N., Shafai, S., Abdullah, M. M., Jaafar, W. S. W. M., ... Cardil, A. (2023). Climate-Change-Driven Droughts and Tree Mortality: Assessing the Potential of UAV-Derived Early Warning Metrics. *Remote Sensing*, *15*(10), Article 10. https://doi.org/10.3390/rs15102627

Ezenne, G. I., Jupp, L., Mantel, S. K., & Tanner, J. L. (2019). Current and potential capabilities of UAS for crop water productivity in precision agriculture. *Agricultural Water Management*, *218*, 158–164. https://doi.org/10.1016/j.agwat.2019.03.034

Fajardo, A., Goodburn, J. M., & Graham, J. (2006). Spatial patterns of regeneration in managed uneven-aged ponderosa pine/Douglas-fir forests of Western Montana, USA. *Forest Ecology and Management*, *223*(1), 255–266. https://doi.org/10.1016/j.foreco.2005.11.022

Finley, K., & Zhang, J. (2019). Climate Effect on Ponderosa Pine Radial Growth Varies with Tree Density and Shrub Removal. *Forests*, *10*(6), Article 6. https://doi.org/10.3390/f10060477

Flannigan, M. D., Wotton, B. M., Marshall, G. A., de Groot, W. J., Johnston, J., Jurko, N., & Cantin, A. S. (2016). Fuel moisture sensitivity to temperature and precipitation: Climate change implications. *Climatic Change*, *134*(1), 59–71. https://doi.org/10.1007/s10584-015-1521-0

Fraser, B. T., & Congalton, R. G. (2021). Monitoring Fine-Scale Forest Health Using Unmanned

Aerial Systems (UAS) Multispectral Models. *Remote Sensing*, *13*(23), Article 23. https://doi.org/10.3390/rs13234873
Gao, B. (1996). NDWI—A normalized difference water index for remote sensing of vegetation liquid water from space. *Remote Sensing of Environment*, *58*(3), 257–266. https://doi.org/10.1016/S0034-4257(96)00067-3
Gao, D., Joseph, J., Werner, R. A., Brunner, I., Zürcher, A., Hug, C., Wang, A., Zhao, C., Bai, E., Meusburger, K., Gessler, A., & Hagedorn, F. (2021). Drought alters the carbon footprint of trees in soils—Tracking the spatio-temporal fate of 13C-labelled assimilates in the soil of an old-growth pine forest. *Global Change Biology*, *27*(11), 2491–2506. https://doi.org/10.1111/gcb.15557
Garza, B. N., Ancona, V., Enciso, J., Perotto-Baldivieso, H. L., Kunta, M., & Simpson, C. (2020). Quantifying Citrus Tree Health Using True Color UAV Images. *Remote Sensing*, *12*(1), Article 1. https://doi.org/10.3390/rs12010170
Gergel, D. R., Nijssen, B., Abatzoglou, J. T., Lettenmaier, D. P., & Stumbaugh, M. R. (2017). Effects of climate change on snowpack and fire potential in the western USA. *Climatic Change*, *141*(2), 287–299. https://doi.org/10.1007/s10584-017-1899-y
Govi, D., Pappalardo, S. E., De Marchi, M., & Meggio, F. (2024). From Space to Field: Combining Satellite, UAV and Agronomic Data in an Open-Source Methodology for the Validation of NDVI Maps in Precision Viticulture. *Remote Sensing*, *16*(5), Article 5. https://doi.org/10.3390/rs16050735
Groover, A. (2017). Age-Related Changes in Tree Growth and Physiology. In John Wiley & Sons, Ltd (Ed.), *eLS* (1st ed., pp. 1–7). Wiley. https://doi.org/10.1002/9780470015902.a0023924
Grulke, N., Maxfield, J., Riggan, P., & Schrader-Patton, C. (2020). Pre-Emptive Detection of Mature Pine Drought Stress Using Multispectral Aerial Imagery. *Remote Sensing*, *12*(14), Article 14. https://doi.org/10.3390/rs12142338
Grybas, H., & Congalton, R. G. (2021). A Comparison of Multi-Temporal RGB and Multispectral UAS Imagery for Tree Species Classification in Heterogeneous New Hampshire Forests. *Remote Sensing*, *13*(13), Article 13. https://doi.org/10.3390/rs13132631
Hanna, L., Tinkham, W. T., Battaglia, M. A., Vogeler, J. C., Ritter, S. M., & Hoffman, C. M. (2024). Characterizing heterogeneous forest structure in ponderosa pine forests via UAS-derived structure from motion. *Environmental Monitoring and Assessment*, *196*(6), 530. https://doi.org/10.1007/s10661-024-12703-1
Harvey, B. J., Donato, D. C., & Turner, M. G. (2016). Burn me twice, shame on who? Interactions between successive forest fires across a temperate mountain region. *Ecology*, *97*(9), 2272–2282. https://doi.org/10.1002/ecy.1439
Hijmans R (2024). terra: Spatial Data Analysis. R package version 1.7-71. https://CRAN.R-project.org/package=terra
Housman, I. W., Chastain, R. A., & Finco, M. V. (2018). An Evaluation of Forest Health Insect and Disease Survey Data and Satellite-Based Remote Sensing Forest Change Detection Methods: Case Studies in the United States. *Remote Sensing*, *10*(8), Article 8. https://doi.org/10.3390/rs10081184
Jemaa, H., Bouachir, W., Leblon, B., LaRocque, A., Haddadi, A., & Bouguila, N. (2023). UAV-Based Computer Vision System for Orchard Apple Tree Detection and Health Assessment. *Remote Sensing*, *15*(14), Article 14. https://doi.org/10.3390/rs15143558
Jolly, W. M., & Hadlow, A. M. (2012). A comparison of two methods for estimating conifer live foliar moisture content. *International Journal of Wildland Fire*, *21*(2), 180. https://doi.org/10.1071/WF11015
Joseph, J., Luster, J., Bottero, A., Buser, N., Baechli, L., Sever, K., & Gessler, A. (2021). Effects of drought on nitrogen uptake and carbon dynamics in trees. *Tree Physiology*, *41*(6), 927–943. https://doi.org/10.1093/treephys/tpaa146

Keyes, Christopher R. 2006. Foliar Moisture Contents of North American Conifers. In: Andrews, Patricia L.; Butler, Bret W., comps. 2006. Fuels Management-How to Measure Success: Conference Proceedings. 28-30 March 2006; Portland, OR. Proceedings RMRS-P-41. Fort Collins, CO: U.S. Department of Agriculture, Forest Service, Rocky Mountain Research Station. p. 395-399

Kreuzwieser, J., & Gessler, A. (2010). Global climate change and tree nutrition: Influence of water availability. *Tree Physiology*, *30*(9), 1221–1234. https://doi.org/10.1093/treephys/tpq055

Lad, L. E., Tinkham, W. T., Sparks, A. M., & Smith, A. M. S. (2023). Evaluating Predictive Models of Tree Foliar Moisture Content for Application to Multispectral UAS Data: A Laboratory Study. *Remote Sensing*, *15*(24), Article 24. https://doi.org/10.3390/rs15245703

Lentile, L. B., Holden, Z. A., Smith, A. M. S., Falkowski, M. J., Hudak, A. T., Morgan, P., Lewis, S. A., Gessler, P. E., & Benson, N. C. (2006). Remote sensing techniques to assess active fire characteristics and post-fire effects. *International Journal of Wildland Fire*, *15*(3), 319. https://doi.org/10.1071/WF05097

Littell, J. S., Peterson, D. L., Riley, K. L., Liu, Y., & Luce, C. H. (2016). A review of the relationships between drought and forest fire in the United States. *Global Change Biology*, *22*(7), 2353–2369. https://doi.org/10.1111/gcb.13275

Liu, J., Gao, L., Yuan, F., Guo, Y., & Xu, X. (2019). Climate Change Made Major Contributions to Soil Water Storage Decline in the Southwestern US during 2003–2014. *Water*, *11*(9), Article 9. https://doi.org/10.3390/w11091947

Marques, P., Pádua, L., Sousa, J., & Fernandes-Silva, A. (2023). Assessing the Water Status and Leaf Pigment Content of Olive Trees: Evaluating the Potential and Feasibility of Unmanned Aerial Vehicle Multispectral and Thermal Data for Estimation Purposes. *Remote Sensing*, *15*, 4777. https://doi.org/10.3390/rs15194777

Mast, J. N., Veblen, T. T., & Linhart, Y. B. (1998). Disturbance and climatic influences on age structure of ponderosa pine at the pine/grassland ecotone, Colorado Front Range. *Journal of Biogeography, 25*(4), 743–755. https://doi.org/10.1046/j.1365-2699.1998.2540743.x

Matthews, S. (2010). Effect of drying temperature on fuel moisture content measurements. *International Journal of Wildland Fire, 19*(6), 800. https://doi.org/10.1071/wf08188

Näsi, R., Honkavaara, E., Blomqvist, M., Lyytikäinen-Saarenmaa, P., Hakala, T., Viljanen, N., Kantola, T., & Holopainen, M. (2018). Remote sensing of bark beetle damage in urban forests at individual tree level using a novel hyperspectral camera from UAV and aircraft. *Urban Forestry & Urban Greening*, *30*, 72–83. https://doi.org/10.1016/j.ufug.2018.01.010

Nauslar, N. J., Hatchett, B. J., Brown, T. J., Kaplan, M. L., & Mejia, J. F. (2019). Impact of the North American monsoon on wildfire activity in the southwest United States. *International Journal of Climatology*, *39*(3), 1539–1554. https://doi.org/10.1002/joc.5899

North, M., Stine, P., O'Hara, K., Zielinski, W., & Stephens, S. (2009). An ecosystem management strategy for Sierran mixed-conifer forests. *Gen. Tech. Rep. PSW-GTR-220 (Second Printing, with Addendum). Albany, CA: U.S. Department of Agriculture, Forest Service, Pacific Southwest Research Station. 49 p*, *220*. https://doi.org/10.2737/PSW-GTR-220

Pádua, L., Marques, P., Martins, L., Sousa, A., Peres, E., & Sousa, J. J. (2020). Monitoring of Chestnut Trees Using Machine Learning Techniques Applied to UAV-Based Multispectral Data. *Remote Sensing*, *12*(18), Article 18. https://doi.org/10.3390/rs12183032

Park Williams, A., Allen, C. D., Macalady, A. K., Griffin, D., Woodhouse, C. A., Meko, D. M., Swetnam, T. W., Rauscher, S. A., Seager, R., Grissino-Mayer, H. D., Dean, J. S., Cook, E. R., Gangodagamage, C., Cai, M., & McDowell, N. G. (2013). Temperature as a potent driver of regional forest drought stress and tree mortality. *Nature Climate Change*, *3*(3), 292–297. https://doi.org/10.1038/nclimate1693

Philpot, C.W. (1965). Diurnal fluctuation in moisture content of ponderosa pine and whiteleaf manzanita leaves. USDA Forest Service Research Note PSW-RN-67. 7 p.

Philpot, C. W., Mutch, R.W. (1971). The seasonal trends in moisture content, ether extractives, and energy of ponderosa pine and Douglas-fir needles. Res. Pap. INT-RP-102. Ogden, UT: USDA Forest Service, Intermountain Forest and Range Experiment Station. 21 p.

Pebesma, E., 2018. Simple Features for R: Standardized Support for Spatial Vector Data. *The R Journal, 10*(1), 439-446. https://doi.org/10.32614/RJ-2018-009

Peltier, D. M. P., Fell, M., & Ogle, K. (2016). Legacy effects of drought in the southwestern United States: A multi-species synthesis. *Ecological Monographs*, *86*(3), 312–326. https://doi.org/10.1002/ecm.1219

Pérez-Rodríguez, L. A., Quintano, C., Marcos, E., Suarez-Seoane, S., Calvo, L., & Fernández-Manso, A. (2020). Evaluation of Prescribed Fires from Unmanned Aerial Vehicles (UAVs) Imagery and Machine Learning Algorithms. *Remote Sensing*, *12*(8), Article 8. https://doi.org/10.3390/rs12081295

Pierce, L. L., Running, S. W., & Riggs, G. A. (1990). Remote detection of canopy water stress in coniferous forests using the NS001 Thematic Mapper simulator and the thermal infrared multispectral scanner. *Photogrammetric Engineering and Remote Sensing*, *56*(5), 579–586.

Plowright A (2024). _ForestTools: Tools for Analyzing Remote Sensing Forest Data_. R package version 1.0.2, <https://CRAN.R-project.org/package=ForestTools>.

R Core Team (2023). R: A Language and Environment for Statistical Computing. R Foundation for Statistical Computing, Vienna, Austria. <https://www.R-project.org/>.

Rautiainen, M., Lukeš, P., Homolová, L., Hovi, A., Pisek, J., & Mõttus, M. (2018). Spectral Properties of Coniferous Forests: A Review of In Situ and Laboratory Measurements. *Remote Sensing*, *10*(2), Article 2. https://doi.org/10.3390/rs10020207

Rock, B. N., Williams, D. L., Moss, D. M., Lauten, G. N., & Kim, M. (1994). High-spectral resolution field and laboratory optical reflectance measurements of red spruce and eastern hemlock needles and branches. *Remote Sensing of Environment*, *47*(2), 176–189. https://doi.org/10.1016/0034-4257(94)90154-6

Rouse, J. W., Haas, R. H., Schell, J. A., & Deering, D. W. (1974). Monitoring vegetation systems in the Great Plains with ERTS. https://ntrs.nasa.gov/citations/19740022614

Roussel J (2024). lasR: Fast and Pipeable Airborne LiDAR Data Tools. R package version 0.5.6, https://github.com/r-lidar/lasR

Roussel, J.R., Auty, D., Coops, N. C., Tompalski, P., Goodbody, T. R. H., Sánchez Meador, A., Bourdon, J.F., De Boissieu, F., Achim, A. (2020). lidR: An R package for analysis of Airborne Laser Scanning (ALS) data. *Remote Sensing of Environment*, *251*, 112061. https://doi.org/10.1016/j.rse.2020.112061

Roussel, J. R., Auty, D. (2024). Airborne LiDAR Data Manipulation and Visualization for Forestry Applications. R package version 4.1.0. https://cran.r-project.org/package=lidR

Ruthrof, K. X., Fontaine, J. B., Matusick, G., Breshears, D. D., Law, D. J., Powell, S., & Hardy, G. (2016). How drought-induced forest die-off alters microclimate and increases fuel loadings and fire potentials. *International Journal of Wildland Fire*, *25*(8), 819–830. https://doi.org/10.1071/WF15028

Ryan, K. C., Knapp, E. E., & Varner, J. M. (2013). Prescribed fire in North American forests and woodlands: History, current practice, and challenges. *Frontiers in Ecology and the Environment*, *11*(s1), e15–e24. https://doi.org/10.1890/120329

Ryan, M. G. (2011). Tree responses to drought. *Tree Physiology*, *31*(3), 237–239. https://doi.org/10.1093/treephys/tpr022

Simonin, K., Kolb, T. E., Montes-Helu, M., & Koch, G. W. (2006). Restoration thinning and influence of tree size and leaf area to sapwood area ratio on water relations of Pinus ponderosa. *Tree Physiology*, *26*(4), 493–503. https://doi.org/10.1093/treephys/26.4.493

Sohn, J. A., Saha, S., & Bauhus, J. (2016). Potential of forest thinning to mitigate drought stress: A meta-analysis. *Forest Ecology and Management*, *380*, 261–273.

https://doi.org/10.1016/j.foreco.2016.07.046
Sparks, A., Kolden, C., Talhelm, A., Smith, A., Apostol, K., Johnson, D., & Boschetti, L. (2016). Spectral Indices Accurately Quantify Changes in Seedling Physiology Following Fire: Towards Mechanistic Assessments of Post-Fire Carbon Cycling. *Remote Sensing, 8*(7), 572. https://doi.org/10.3390/rs8070572
Steckel, M., Moser, W. K., del Río, M., & Pretzsch, H. (2020). Implications of Reduced Stand Density on Tree Growth and Drought Susceptibility: A Study of Three Species under Varying Climate. *Forests, 11*(6), Article 6. https://doi.org/10.3390/f11060627
Stephens, S. L., Collins, B. M., Fettig, C. J., Finney, M. A., Hoffman, C. M., Knapp, E. E., North, M. P., Safford, H., & Wayman, R. B. (2018). Drought, Tree Mortality, and Wildfire in Forests Adapted to Frequent Fire. *BioScience*, *68*(2), 77–88. https://doi.org/10.1093/biosci/bix146
Stevens-Rumann, C. S., & Morgan, P. (2019). Tree regeneration following wildfires in the western US: A review. *Fire Ecology*, *15*(1), 15. https://doi.org/10.1186/s42408-019-0032-1
Stout, D. L., & Sala, A. (2003). Xylem vulnerability to cavitation in Pseudotsuga menziesii and Pinus ponderosa from contrasting habitats. *Tree Physiology*, *23*(1), 43–50. https://doi.org/10.1093/treephys/23.1.43
Swayze, N. C., Tinkham, W. T., Vogeler, J. C., & Hudak, A. T. (2021). Influence of flight parameters on UAS-based monitoring of tree height, diameter, and density. *Remote Sensing of Environment*, *263*, 112540. https://doi.org/10.1016/j.rse.2021.112540
Tinkham, W. T., & Swayze, N. C. (2021). Influence of Agisoft Metashape Parameters on UAS Structure from Motion Individual Tree Detection from Canopy Height Models. *Forests, 12*(2), Article 2. https://doi.org/10.3390/f12020250
Tinkham, W. T., Swayze, N. C., Hoffman, C. M., Lad, L. E., & Battaglia, M. A. (2022). Modeling the Missing DBHs: Influence of Model Form on UAV DBH Characterization. *Forests*, *13*(12), Article 12. https://doi.org/10.3390/f13122077
Tinkham, W.T., Woolsey, G.A. (2024). Influence of Structure for Motion Algorithm Parameters on Metrics of Individual Tree Detection Accuracy and Precision. *Remote Sensing*, *16*(20), 3844. https://doi.org/10.3390/rs16203844
User guide for micasense sensors – micasense knowledge base. (n.d.). https://support.micasense.com/hc/en-us/articles/360039671254-User-Guide-for-MicaSense-Sensors
Vogelmann, J. E., Tolk, B., & Zhu, Z. (2009). Monitoring forest changes in the southwestern United States using multitemporal Landsat data. *Remote Sensing of Environment*, *113*(8), 1739–1748. https://doi.org/10.1016/j.rse.2009.04.014
Wainwright, H. M., Steefel, C., Trutner, S. D., Henderson, A. N., Nikolopoulos, E. I., Wilmer, C. F., Chadwick, K. D., Falco, N., Schaettle, K. B., Brown, J. B., Steltzer, H., Williams, K. H., Hubbard, S. S., & Enquist, B. J. (2020). Satellite-derived foresummer drought sensitivity of plant productivity in Rocky Mountain headwater catchments: Spatial heterogeneity and geological-geomorphological control. *Environmental Research Letters*, *15*(8), 084018. https://doi.org/10.1088/1748-9326/ab8fd0
Williams, A. P., Cook, E. R., Smerdon, J. E., Cook, B. I., Abatzoglou, J. T., Bolles, K., Baek, S. H., Badger, A. M., & Livneh, B. (2020). Large contribution from anthropogenic warming to an emerging North American megadrought. *Science*, *368*(6488), 314–318. https://doi.org/10.1126/science.aaz9600
Woolsey, G. (2024). *cloud2trees: Point Cloud Data to Forest Inventory Tree List*. R package version 0.1.0. Retrieved from https://CRAN.R-project.org/package=cloud2trees
Young, D. J. N., Estes, B. L., Gross, S., Wuenschel, A., Restaino, C., & Meyer, M. D. (2023). Effectiveness of forest density reduction treatments for increasing drought resistance of ponderosa pine growth. *Ecological Applications: A Publication of the Ecological Society of America*, *33*(4), e2854. https://doi.org/10.1002/eap.2854

Zarco-Tejada, P. J., González-Dugo, V., & Berni, J. A. J. (2012). Fluorescence, temperature and narrow-band indices acquired from a UAV platform for water stress detection using a micro-hyperspectral imager and a thermal camera. *Remote Sensing of Environment*, *117*, 322–337. https://doi.org/10.1016/j.rse.2011.10.007

Zhang, J., Finley, K. A., Johnson, N. G., & Ritchie, M. W. (2019). Lowering Stand Density Enhances Resiliency of Ponderosa Pine Forests to Disturbances and Climate Change. *Forest Science, 65*(4), 496–507. https://doi.org/10.1093/forsci/fxz006

Appendix A: Contact Information for Key Project Personnel

Lauren E. Lad
Forest and Rangeland Stewardship
Colorado State University
1472 Campus Delivery
Fort Collins, CO 80523-1472
Lauren.Lad@colostate.edu

Camille S. Stevens-Rumann
Associate Professor
Forest and Rangeland Stewardship
Colorado State University
1472 Campus Delivery
Fort Collins, CO 80523-1472
C.Stevens-Rumann@colostate.edu

Appendix B: List of Completed/Planned Scientific/Technical Publications/Science Delivery Products

Graduate Dissertation:
Lad, L. E. (*In prep.)*. Predictive models of individual tree health: The utility of uncrewed aerial system data to inform forest management. Ph.D. Dissertation, Colorado State University, Fort Collins, CO.

Conference Presentations:
1. Tinkham, W., Woolsey, G., **Lad., L.** (2024, September). *UAS Data Collection for Ponderosa Pine Monitoring*. [Conference Presentation]. 2024 Society of American Foresters National Convention, Loveland, CO.
2. **Lad, L.,** Tinkham, W., Stevens-Rumann, C. (2024, September). *UAS Classification of Conifer Drought Status – Identifying Target Trees for Forest Management.* [Conference Presentation]. 2024 Society of American Foresters National Convention, Loveland, CO.

Publications:
1. **Lad, L. E.,** Tinkham, W. T., Sparks, A. M., & Smith, A. M. S. (2023). Evaluating Predictive Models of Tree Foliar Moisture Content for Application to Multispectral UAS Data: A Laboratory Study. Remote Sensing, 15(24), Article 24. **https://doi.org/10.3390/rs15245703**

Summary Guide:
We have created a one-page summary guide providing the necessary data collection, processing, and analysis steps to repeat this project. This summary guide can be used to replicate the study in additional forests and forest types. This summary guide will be shared following journal publication of this project's manuscript.

Appendix C: Metadata

The metadata for this project describe the collected tree foliar moisture contents (FMC) from the field sites. Tree FMC was collected between 1100 and 1300 at two sites across four dates using multiple needle samples from each tree. The metadata also describe the UAS image collection process which took place as close to 1200 as weather conditions allowed.

The raw data and metadata will be uploaded to the US Forest Service Research Data Archive (USFS-RDA) following journal publication. Pre-processed data from this project will also be made available upon request.